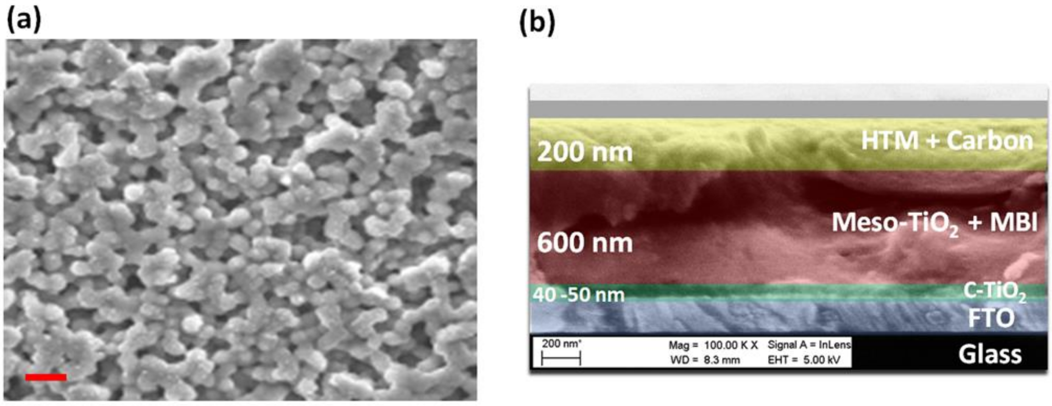

Supplementary Figure 1 Morphological properties of MBI solar cells

(a) Surface morphology of MBI deposited on FTO/C-TiO_2/Mesoporous-TiO_2 substrate. The red scale represents 1 µm (b) Solar cell device crossection showing dense ≈ 600 nm thicker MBI absorber film used in solar cells

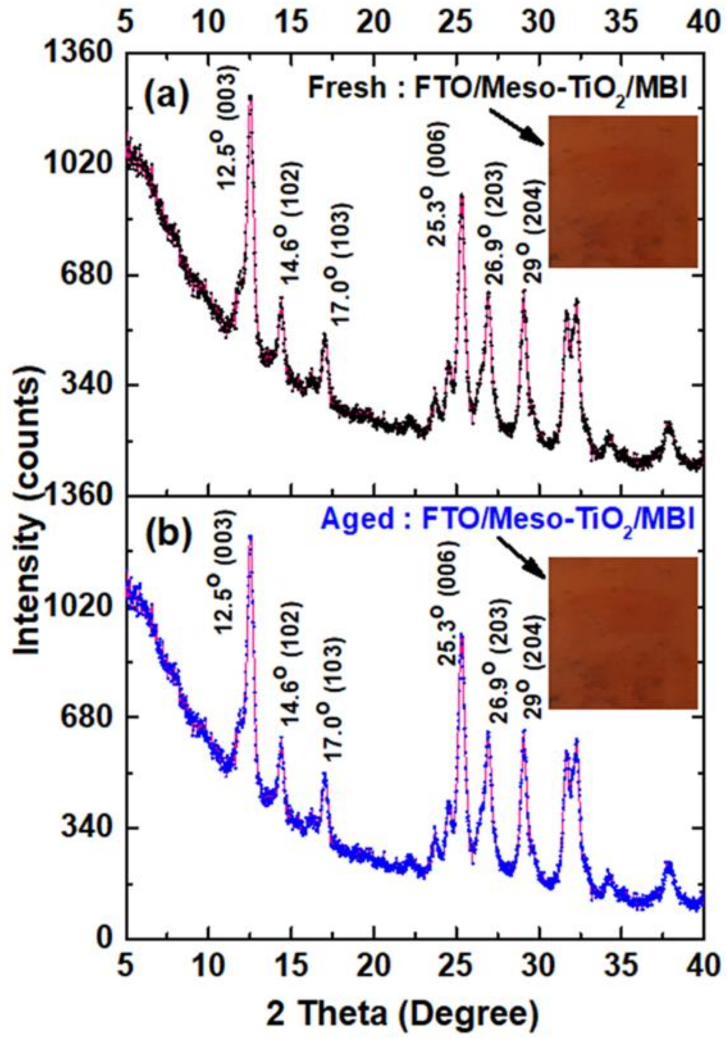

Supplementary Figure 2 Crystalline properties of fresh and aged MBI films. X-ray diffraction pattern for (a) fresh MBI (red curve) films deposited on FTO/Mesoporous TiO_2 substrate (b) aged film (blue curve) under continuous 1 sun illumination for 30 days (720 hours). Shows no trace of degradation in crystalline quality of the MBI films after aging.

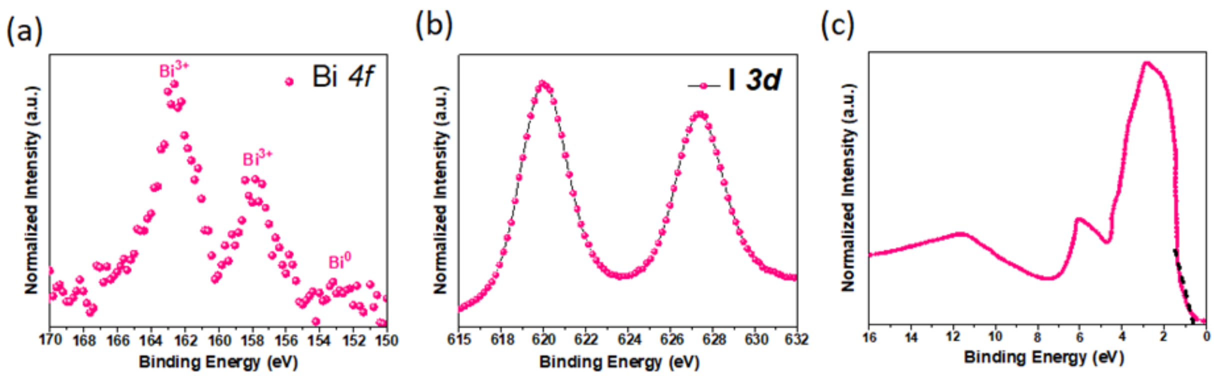

Supplementary Figure 3 Chemical analysis of MBI films

(a) X-ray photoelectron sprectroscopy core level spectra of Bi *4f* (b) I *3d*. (c) Valence band spectrum for MBI ($(CH_3NH_3)_3Bi_2I_9$) film (to mimics the device architecture all characterization done on MBI films deposited on FTO/Meso-TiO_2 substrate)

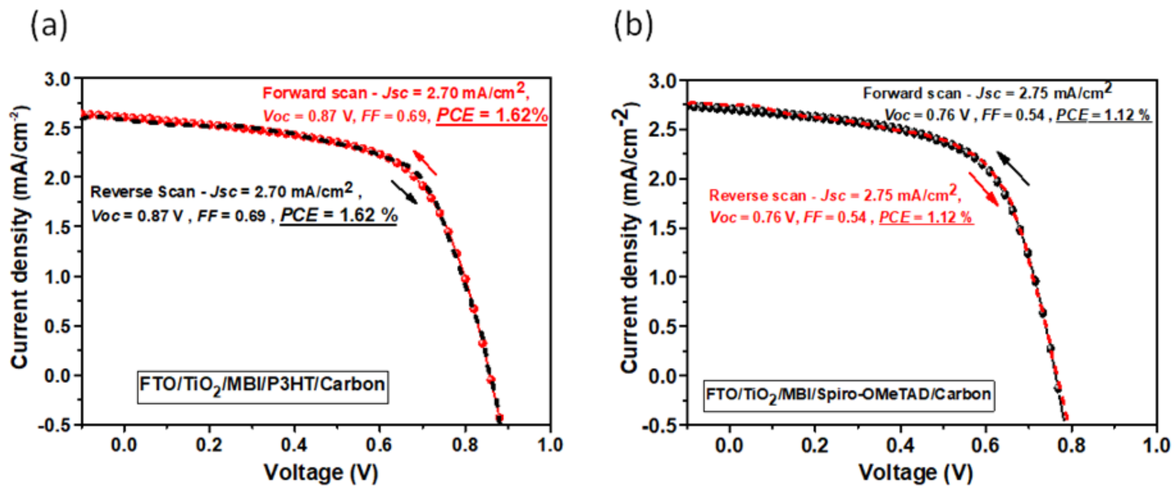

Supplementary Figure 4. Hysteresis behaviour of MBI solar cells.

(a) prepared using P3HT and (b) Spiro-OMeTAD as hole transport layer. (F) – forward arrow and (R) – reverse arrow indicates forward and reverse scan respectively. All devices were subjected to slow scan speed of 0.10 mV/s and measured under 1 sun illumination.

Supplementary Table 1. Hysteresis parameters of champion MBI solar cells

(a) Hysteresis of MBI solar cells employing P3HT and (b) Spiro-OMeTAD as hole transport layer. (F) and (R) indicates forward and reverse scan respectively.

Solar cells made with different HTM	*Jsc* (mA/cm^2)	Voc (V)	FF (%)	PCE (%)
MBI/Spiro-OMeTAD (F)	2.75	0.76	0.54	1.12
MBI/Spiro-OMeTAD (R)	2.75	0.76	0.54	1.12
MBI/P3HT (F)	2.70	0.87	0.69	1.62
MBI/P3HT (R)	2.70	0.87	0.69	1.62

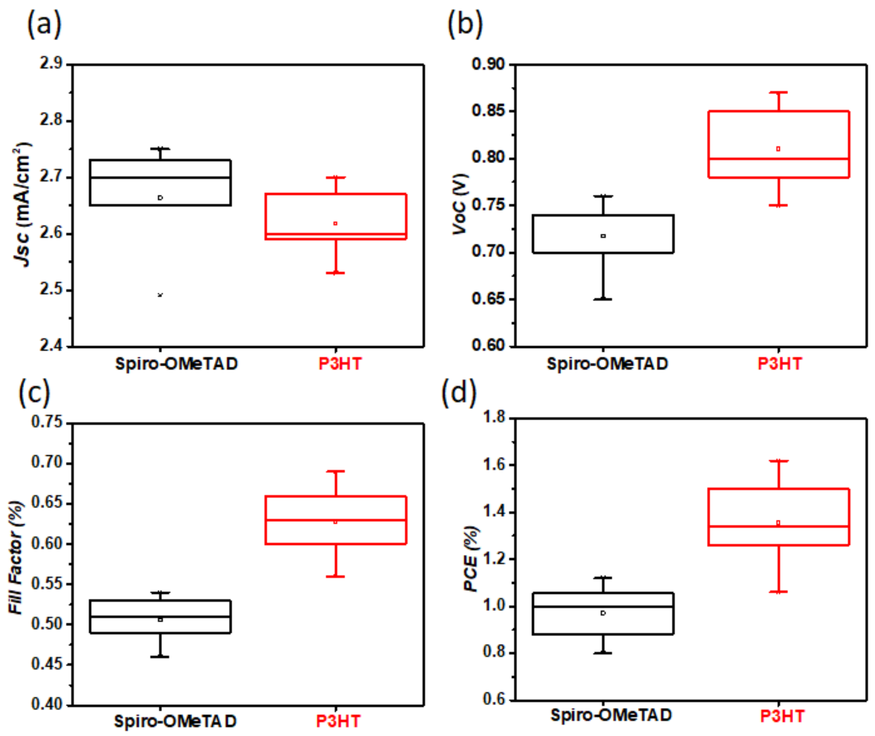

Supplementary Figure 5. Statistics of photovoltaic characteristics of MBI solar cells made employing different hole transport layers.

(a) *Jsc* (mA/cm^2) (b) Voc (V) (c) FF and (d) power conversion efficiency (PCE) for 27 devices made using Spiro-OMeTAD and P3HT hole transport layers. Showing average device efficiency of 1.0 % and 1.4% for devices made employing Spiro-OMeTAD (black) and P3HT (red) hole transport layers respectively.

Supplementary Table 2. Energy levels of hole transport layers employed in MBI solar cell. The highest occupied molecular orbital (HOMO) , Lowest unoccupied molecular orbital (LUMO) levels of P3HT and Spiro-OMeTAD hole transport materials.

Energy levels	Spiro-OMeTAD[1]	P3HT[2]
HOMO	-2.22 eV	- 3.50 eV
LUMO	-5.11 eV	-5.20 eV

Supplementary References

[1] Urieta-Mora, J., García-Benito, I., Molina-Ontoria, A., Martín, N., Hole transporting materials for perovskite solar cells: a chemical approach. Chem. Soc. Rev., **47,** 8541-8571 (2018)

[2] Petr, P. K., Beate, B., Andrey, E. R., Barry, C. T. Optimization and simplification of polymer–fullerene solar cells through polymer and active layer design. Polymer, **54,** 20, 5267-5298 (2013)